(12) INTERNATIONAL APPLICATION PUBLISHED UNDER THE PATENT COOPERATION TREATY (PCT)

(19) World Intellectual Property Organization
International Bureau

(43) International Publication Date
4 October 2012 (04.10.2012)

WIPO | PCT

(10) International Publication Number
WO 2012/129704 A1

(51) International Patent Classification:
G01T 1/22 (2006.01) *G01T 1/29* (2006.01)
G01T 1/167 (2006.01) *G21C 17/06* (2006.01)

(21) International Application Number:
PCT/CA2012/050206

(22) International Filing Date:
30 March 2012 (30.03.2012)

(25) Filing Language: English

(26) Publication Language: English

(30) Priority Data:
61/469,569 30 March 2011 (30.03.2011) US
61/469,578 30 March 2011 (30.03.2011) US

(71) Applicant *(for all designated States except US)*: **AECL ATOMIC ENERGY OF CANADA LIMITED** [CA/CA]; Chalk River Laboratories, Chalk River, Ontario K0J 1J0 (CA).

(72) Inventors; and

(75) Inventors/Applicants *(for US only)*: **SUR, Bhaskar** [IN/CA]; 9 Highland Crescent, Deep River, Ontario K0J 1P0 (CA). **ANGHEL, Vinicius N. P.** [CA/CA]; 72 Beach Avenue, Deep River, Ontario K0J 1P0 (CA). **JOHNSTON, James** [CA/CA]; 529 Lacroche Crescent, Chalk River, Ontario K0J 1J0 (CA). **VERDUN, Toban** [CA/CA]; 114 Deep River Road, Deep River, Ontario K0J 1P0 (CA).

(74) Agent: **BERESKIN & PARR LLP/S.E.N.C.R.L., S.R.L.**; 40 King Street West, 40th Floor, Toronto, Ontario M5H 3Y2 (CA).

(81) Designated States *(unless otherwise indicated, for every kind of national protection available)*: AE, AG, AL, AM, AO, AT, AU, AZ, BA, BB, BG, BH, BR, BW, BY, BZ, CA, CH, CL, CN, CO, CR, CU, CZ, DE, DK, DM, DO, DZ, EC, EE, EG, ES, FI, GB, GD, GE, GH, GM, GT, HN, HR, HU, ID, IL, IN, IS, JP, KE, KG, KM, KN, KP, KR, KZ, LA, LC, LK, LR, LS, LT, LU, LY, MA, MD, ME, MG, MK, MN, MW, MX, MY, MZ, NA, NG, NI, NO, NZ, OM, PE, PG, PH, PL, PT, QA, RO, RS, RU, RW, SC, SD, SE, SG, SK, SL, SM, ST, SV, SY, TH, TJ, TM, TN, TR, TT, TZ, UA, UG, US, UZ, VC, VN, ZA, ZM, ZW.

(84) Designated States *(unless otherwise indicated, for every kind of regional protection available)*: ARIPO (BW, GH, GM, KE, LR, LS, MW, MZ, NA, RW, SD, SL, SZ, TZ, UG, ZM, ZW), Eurasian (AM, AZ, BY, KG, KZ, MD, RU, TJ, TM), European (AL, AT, BE, BG, CH, CY, CZ, DE, DK, EE, ES, FI, FR, GB, GR, HR, HU, IE, IS, IT, LT, LU, LV, MC, MK, MT, NL, NO, PL, PT, RO, RS, SE, SI, SK, SM, TR), OAPI (BF, BJ, CF, CG, CI, CM, GA, GN, GQ, GW, ML, MR, NE, SN, TD, TG).

Published:

— *with international search report (Art. 21(3))*

(54) Title: QUANTITATIVE CERENKOV RADIATION VIEWING METHODS AND SYSTEMS

FIG. 3

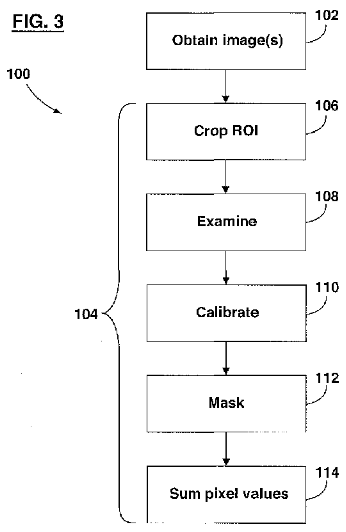

(57) Abstract: A method of viewing Cerenkov radiation being emitted from an object includes obtaining at least one image of the object, and calculating an intensity value for at least a portion of the image. A region of interest may be defined within the image, and an intensity value may be calculated for the region of interest. A system for viewing Cerenkov radiation being emitted from an object includes a lens, a UV filter, an image intensifier device and an image sensor device.

WO 2012/129704 A1

TITLE: QUANTITATIVE CERENKOV RADIATION VIEWING METHODS AND SYSTEMS

CROSS-REFERENCE TO RELATED APPLICATIONS

[0001] This application claims priority to U.S. Provisional Application No. 61/469,569 filed on March 30, 2011 and U.S. Provisional Application No. 61/469,578 filed on March 30, 2011. The entire contents of each are hereby incorporated herein by reference.

FIELD

[0002] This specification relates to methods of and systems for quantitatively determining the radioactivity of objects, including, for example, irradiated fuel bundles of nuclear reactors.

BACKGROUND

[0003] The following paragraphs are not an admission that anything discussed in them is prior art or part of the knowledge of persons skilled in the art.

[0004] Cerenkov radiation is electromagnetic radiation emitted when a charged particle passes through a dielectric medium at a speed greater than the phase velocity of light in that medium. When stored underwater, used nuclear fuel bundles emanate Cerenkov light, and the intensity of the blue glow is related to level of radioactivity of each fuel bundle. The Cerenkov radiation being emitted from the fuel can provide an indication of how long the fuel was irradiated inside the nuclear reactor core (burn-up), and how long it has been out of the core (cooling time).

INTRODUCTION

[0005] The following is intended to introduce the reader to this specification but not to define any invention.

[0006] The teachings herein relate to the quantitative measurement of radioactivity of objects, including, for example, irradiated fuel bundles of nuclear reactors.

[0007] In a first aspect, a method of viewing Cerenkov radiation being emitted from an object can include: obtaining at least one image of the object; and calculating an intensity value for at least a portion of the image.

[0008] The method can further include, prior to the step of calculating, defining a region of interest within the image, and wherein the step of calculating includes calculating an intensity value for the region of interest.

[0009] The step of defining can include cropping the image. An external area of the image relative to the object can be cropped. An internal area of the image relative to the object can be cropped.

[0010] The method can further include, prior to the step of calculating, examining the image and correcting for at least one of noise, underexposure and overexposure.

[0011] The method can further include, prior to the step of calculating, calibrating the image by adjusting pixel values. The pixel values can be adjusted based on exposure time and gain settings used in the step of obtaining the image. The step of calculating can include summing pixel values for the portion of the image to yield the intensity value.

[0012] The method can further include, prior to the step of calculating, applying a mask to isolate a section of the image. The step of applying can include selecting pixels having an intensity of greater than a predetermined amount of a maximum intensity. The predetermined amount can be about 20%. The step of applying can include selecting pixels within an external region of the object, and the step of calculating can include summing pixel values for the external region. The step of applying can include selecting pixels within an internal region of the object, and the step of calculating can include summing pixel values for the internal region. The step of applying can include determining a tilt angle of the object relative to an optical axis, and correcting the intensity value based on the tilt angle.

[0013] The method can further include determining radioactivity of the object based on the intensity value. The step of determining can include correlating a decay heat value for the object based on the intensity value.

[0014] The step of obtaining can include receiving an image signal from an image sensor device. The step of obtaining can include viewing the object through an image intensifier device coupled to the image sensor device. The method can further include, prior to the step of obtaining, mounting the image sensor device generally at an image plane of the image intensifier device. The step of obtaining can include storing a plurality of images of the object encoded in the image signal into a memory. The step of obtaining can include displaying images encoded in the image signal on a viewfinder. The step of obtaining can include viewing the object through a UV filter.

[0015] The object can include at least one nuclear fuel bundle. The object can include at least one CANDU-type nuclear fuel bundle.

[0016] In a second aspect, a system for viewing Cerenkov radiation being emitted from an object can include: a lens; a UV filter coupled to the lens; an image intensifier device coupled to the UV filter; and an image sensor device coupled to the image intensifier device.

[0017] The image sensor device can be mounted generally at an image plane of the image intensifier device. The image sensor device can include a charge-coupled device (CCD). The image sensor device can include an active pixel sensor. The image sensor device can include a complementary metal-oxide-semiconductor (CMOS) sensor.

[0018] The UV filter can be configured to selectively pass wavelengths associated with Cerenkov radiation. The UV filter can have a pass-band of between about 300 nm and 330 nm.

[0019] The system can further include a processor coupled to the image sensor device, and configured to receive an image signal from the image sensor device. The system can further include a memory coupled to the processor, and configured to store a plurality of images of the object encoded in the image signal. The image signal can be a digital signal. The digital signal can be encoded using Serial Digital Interface protocol or Camera Link protocol. The system can further include a viewfinder coupled to the processor, and configured to display images encoded in the image signal.

[0020] The system can further include an accelerometer coupled to the processor, and configured to detect motion of the system. The processor can be configured to compensate for blurring of the object induced by the motion. The system can further include an audio recorder coupled to the processor, and configured to record an audio note associated with an image encoded in the image signal.

[0021] The processor can be configured to calculate an intensity value for at least a portion of an image encoded in the image signal. The processor can be configured to crop the image to define a region of interest, and the intensity value is calculated for the region of interest. The processor can be configured to examine the region of interest and correct for noise, underexposure or overexposure. The processor can be configured to calibrate the region of interest within the image by adjusting pixel values based on exposure time and gain settings of the image sensor device. The processor can be configured to calculate the intensity value by summing pixel values for the region of interest within the image. The processor can be configured to apply a mask to isolate a section of the region of interest of the image. The processor can be configured to determine a tilt angle of the object relative to an optical axis, and correct the intensity value based on the tilt angle.

[0022] The image intensifier device and the image sensor device can be integrated into a camera unit. The lens, the UV filter, the camera unit and the processor can be integrated into a single device. The system can further include a viewfinder integrated into the single device. The single device can be sized and shaped to be a handheld device. The single device can be battery powered.

[0023] Other aspects and features of the teachings disclosed herein will become apparent, to those ordinarily skilled in the art, upon review of the following description of the specific examples of the specification.

BRIEF DESCRIPTION OF THE DRAWINGS

[0024] The drawings included herewith are for illustrating various examples of articles, methods, and apparatuses of the present specification and are not intended to limit the scope of what is taught in any way. In the drawings:

[0025] FIG. 1A shows a device for viewing and recording Cerenkov radiation.

[0026] FIG. 1B shows the device of FIG. 1A being used by an operator.

[0027] FIG. 1C is a schematic view of the device of FIG. 1A positioned above a nuclear fuel bundle housed underwater.

[0028] FIGS. 2A and 2B are side and end views, respectively, of a CANDU-type nuclear fuel bundle.

[0029] FIG. 3 is a flowchart illustrating method steps.

[0030] FIG. 4A is an end-view image of a CANDU-type nuclear fuel bundle, showing Cerenkov radiation.

[0031] FIG. 4B is an image of the nuclear fuel bundle of FIG. 4A, and in which areas have been cropped to define a region of interest.

[0032] FIG. 5A is a normalized cumulative histogram of pixel values for FIG. 4B.

[0033] FIG. 5B is a plot of average pixel intensity versus shutter speed and gain.

[0034] FIG. 6A shows a user interface displaying the image of FIG. 4B, and in which centers of fuel pins around an outside ring of the fuel bundle are selected.

[0035] FIGS. 6B, 7A and 7B show the image of FIG. 4B, and in which masks have been applied to show selected regions.

[0036] FIG. 8A shows a user interface displaying the image of FIG. 4B, and in which centers of fuel pins around an inner ring of the fuel bundle are selected.

[0037] FIG. 8B is a schematic, side, sectional view of a nuclear fuel bundle.

[0038] FIGS. 9A and 9B are plots of decay heat versus integrated intensity values.

[0039] FIG. 10 is a plot of relative intensity versus cooling time for different fuel bundles.

[0040] FIGS. 11A, 11B and 11C are end-view images of other nuclear fuel bundles, showing Cerenkov radiation.

[0041] FIG. 12A and 12B are schematic and perspective views, respectively, of a system.

DETAILED DESCRIPTION

[0042] Various apparatuses or processes will be described below to provide an example of an embodiment of each claimed invention. No embodiment described below limits any claimed invention and any claimed invention may cover processes or apparatuses that are not described below. The claimed inventions are not limited to apparatuses or processes having all of the features of any one apparatus or process described below or to features common to multiple or all of the apparatuses described below. It is possible that an apparatus or process described below is not an embodiment of any claimed invention. The applicants, inventors or owners reserve all rights that they may have in any invention disclosed in an apparatus or process described below that is not claimed in this document, for example the right to claim such an invention in a continuing application and do not intend to abandon, disclaim or dedicate to the public any such invention by its disclosure in this document.

[0043] A manual Cerenkov viewing device can be used to view the Cerenkov radiation being emitted from used fuel bundles or assemblies, which can be photographed or viewed directly through a viewfinder. In some examples, a manual viewing device can take the form of a hand-held unit that includes an image intensifier tube to amplify the weak Cerenkov emission from the spent fuel, and an ultraviolet (UV) pass filter to permit operation with the room lights on. In other examples, a cooled, UV, charge-coupled device (CCD) camera can be used to obtain digital images of the Cerenkov radiation. However, qualitative assessments with a manual Cerenkov viewing device or the cooled, UV, CCD camera do not provide quantitative information about the burn-up/cooling time of used fuel.

[0044] Quantitative information about burn-up and cooling time can be useful for researchers, operators, and nuclear non-proliferation agencies. In order to develop new types of reactor fuel, or qualify existing fuel types for new or extended uses, researchers may need to determine how much irradiation the fuel has undergone during in-reactor tests. Operators may need to verify the irradiation history of fuel to ensure that it is used in compliance with regulatory and operating limits. Nuclear non-proliferation enforcement agencies (e.g., the International Atomic Energy Agency) may need to verify that the stated inventory of used nuclear fuel is correct and that it has not been tampered with. Quantitative estimation of the gross radioactivity in the used fuel may be desirable in all three cases.

[0045] Methods that can be used for quantitative determination of used nuclear fuel burn-up/cooling time include: (i) a sample of used fuel can be taken to a shielded facility (a "hot-cell") where it can be counted using a highly collimated gamma-ray spectrometer; (ii) a sample of used fuel can be taken to a shielded facility where it can be analyzed chemically; and (iii) a gamma-ray spectrometer or gross gamma radiation field counter can be brought in proximity to the fuel while it is stored underwater.

[0046] Methods (i) and (ii) tend to be intrusive and destructive processes. Consequently, these methods can be time-consuming, labour intensive, and expensive, and it can be impractical to carry out such examinations on a large proportion of the used fuel for any reactor. An *in-situ* gamma detector (method (iii) above) can be difficult to remotely position underwater, and the detection may not be accurate if the gamma detector is too close to the used fuel and saturates, or if too far away from the fuel and the signal is contaminated by gamma rays from adjacent fuel bundles. Also, uranium fuel tends to be self-shielding and therefore external gamma rays may not provide a good indication of the internal radioactivity of the fuel bundle.

[0047] Referring to FIG. 1A, a device 10 can be used to view and obtain images of Cerenkov radiation being emitted from an object, which can be, for example, an irradiated nuclear fuel bundle stored underwater in a spent fuel bay. The device 10 includes a lens 12, which can be, for example, a 105 mm refractive or a 250 mm catadioptic (mirror-lens combination) lens. The lens 12 is coupled to a UV band-pass filter 14 that is configured to suppress ambient visible light. The filter 14 is coupled to a UV-optimized image intensifier 16. The image intensifier 16 can consist of a UV sensitive photocathode, a micro-channel plate and a phosphor viewing screen that amplifies the collected and focused UV light and presents an image in the visible spectrum. The image intensifier 16 is coupled to a camera device 18. The lens 12, the filter 14, the intensifier tube 16 and the camera device 18 can all be aligned along an optical axis 19.

[0048] FIG. 1B shows the device 10 being used by an operator to obtain an image. FIG. 1C shows positioning of the device 10 along a bridge 20, above a fuel bundle 22 housed underwater in a storage bay 24.

[0049] Using methods described herein, the device 10 can provide a quantitative measurement, at approximately the 10% uncertainty level, of the Cerenkov radiation intensity relative to the burn-up and cooling time history of fuel bundles with similar, known geometry and composition.

[0050] By way of background, and referring to FIGS. 2A and 2B, a CANDU-type nuclear fuel bundle 26 can include a plurality of elongate and generally cylindrical fuel pins 28a, 28b, 28c, 28d (in this case, thirty seven fuel pins) arranged radially about a longitudinal axis 30 of the fuel bundle 26. As illustrated, the fuel bundle 26 can include three outer concentric rings of the pins (inner pins 28a, intermediate pins 28b and outer pins 28c) surrounding a center pin (28d). Ends of each of the fuel pins 28a, 28b, 28c, 28d can be welded or otherwise fixed to end plates 32.

[0051] FIG. 3 illustrates an example of a method 100 of viewing Cerenkov radiation being emitted from a fuel bundle. In step 102 of the method 100, at least one image is obtained of the fuel bundle, using, for example, the device 10 of FIG. 1A. Next, image analysis 104 of the at least one image obtained in step 102 can include a number of separate steps.

[0052] According to the examples described herein, the images obtained at step 102 and subjected to image analysis 104 can be 8-bit greyscale images, i.e., a two-dimensional array of numbers or pixels, where the value of each pixel ranges between 0 (black) and 255 (white). The analyzed portion of each image can consist of an array of approximately 150 × 150 pixels, for example. As an assumption, the fuel bundle is considered to be the only source of Cerenkov radiation captured in the image. The image is formed by Cerenkov radiation from the fuel bundle, readout noise and dark current from the camera, as well as reflected and scattered light from the fuel bundle and from ambient incandescent lights. The object of the analysis 104 is to distinguish and measure the intensity of the image component caused by direct Cerenkov radiation from the fuel bundle, in the presence of interference from reflection, scattering and ambient light sources (including other fuel bundles).

[0053] The methodology of the image analysis 104 can address the following issues, which are each described in greater detail further below.

[0054] First, for images of the same fuel bundle, taken with widely different camera exposure times, the greyscale pixel values may not scale linearly with the light intensity integrated over exposure time. On each pixel, the greyscale dependence on exposure can be linear for small values of exposure, and tends to an asymptotic value of 255 with increasing exposure. Noise can obscure the dependence for small values of the exposure. Accordingly, calibration can be carried out to meaningfully compare images containing different combinations of fuel bundle, ambient light sources, gain settings and camera exposure times.

[0055] Second, the position, orientation, and tilt angle of the fuel bundle of interest can be deduced from the image, and used to correct the measured intensities corresponding to the fuel bundle.

[0056] Third, consistent measures of Cerenkov radiation intensity can be obtained for comparison of different fuel bundles. These measures can correct for the bundle orientation and for background caused by reflection and scattering of Cerenkov radiation and ambient light. As described herein, two measures can be implemented: (i) an external integrated intensity, which refers to an orientation-independent relative measure of Cerenkov radiation produced in a small volume outside the fuel bundle; and (ii) an internal integrated intensity, which is a relative measure of Cerenkov radiation produced in an annular space between outer two rings of fuel pins in the bundle.

[0057] FIG. 4A shows an example of a greyscale image with appropriate exposure, and with no irrelevant objects close to a fuel bundle of interest 26. The fuel bundle 26 can be seen in the center of the image. The fuel bundle 26 is tilted, i.e. tilted relative to the optical axis 19 of the device 10 shown in FIG. 1A, so that a small crescent of Cerenkov radiation glow 58 is seen adjacent to the lower left of the fuel bundle. A relatively intense Cerenkov radiation glow 72 can be seen between the pins in the fuel bundle 26. A reflection 60, which is a spurious feature as far as present analysis is concerned, can be seen on the image at a distance from the fuel bundle 26 on the lower left side, coming from the support of the fuel bundle 26.

[0058] Referring again to FIG. 3, in step 106 of the method 100, a region of interest (ROI) of the image containing the fuel bundle and its Cerenkov radiation glow can be defined by cropping the image. Cropping can eliminate the large expanse of black that can be present in the image, which generally contains no useful information. Cropping can also eliminate many irrelevant features, such as the reflection 60 seen at the lower left side of FIG. 4A. Step 106 can be done automatically by processing software carrying out the image analysis 104, or manually by an operator analyzing and selecting areas of an image to be cropped, or a combination of automatic and manual interaction.

[0059] In defining the ROI, an external area of the image relative to the object can be cropped. In this example, which is dependent upon the end structure of the fuel bundle 26 as shown in FIG. 2B, the ROI can be established by first defining an outer circle approximately twice the radius of the fuel bundle, concentric with the circular outline of the fuel bundle endplate. The factor of two was selected by the inventors empirically to capture the direct glow from the fuel bundle and provide room for the slight elliptical outline of the endplate and Cerenkov radiation glow, which results from the fuel bundle not being perfectly aligned with the optical axis of the device. The image is thereby cropped so that all data outside of the outer circle area is eliminated from the image.

[0060] In defining the ROI, an internal area of the image relative to the object can also be cropped. With CANDU-type fuel bundles, the central pin may be removed in some situations so that the bundle can be threaded onto a stringer. During storage, a handling fixture can be mounted through the central opening presented by the missing center pin. The handling fixture can reflect ambient bay lighting, creating features in the image that are not attributable to Cerenkov radiation. Accordingly, in this particular example, the ROI can be further refined by defining an inner circle approximately equal in radius to the circular region containing the inner pins 28a, adjacent to the intermediate pins 28b (see FIG. 2B). The image is thereby masked so that all data inside of the inner circle area is eliminated from the image, thus avoiding any light reflected by the handling fixture. The cropped image corresponding to FIG. 4A is shown in FIG. 4B, in which an external area 62 and an internal area 64 relative to the fuel bundle 26 are cropped.

[0061] Referring again to FIG. 3, in step 108 of the method 100, the image can be examined for anomalies that affect its quality, such as noise, underexposure and overexposure. Overexposure results in saturation and subsequently to underestimation of the brightness of the Cerenkov radiation glow. Overexposure, underexposure and noise can increase the uncertainty in the results. Step 108 can be done automatically by processing software carrying out the image analysis 104, or manually by an operator examining an image, or a combination of automatic and manual examination. In step 108, images suffering from noise, underexposure or overexposure can be adjusted or discarded from the image analysis 104.

[0062] For example, a cumulative histogram of the greyscale, obtained from the cropped ROI of the image, can be used as a tool for step 108. The plot in FIG. 5A shows a normalized cumulative histogram of the greyscale pixel values for FIG. 4B. The portions outside the ROI are not considered in constructing the cumulative histogram. The plot indicates that the pixel values are distributed between approximately 25 and 175 (on a scale from 0 to 255). None of the pixels are brighter than 175, confirming that the image is not overexposed. The median brightness is approximately 70, indicating that the image is not underexposed. Thus, the image in FIG. 4B is considered suitable for further analysis.

[0063] A calibration scaling function can be obtained in order to compare images of different fuel bundles, ambient light sources, camera gain settings and camera exposure times. As used herein, the term "gain" refers to an amplification factor of the intensity generated by the image intensifier 16.

[0064] For images of the same object, the greyscale pixel values may not scale linearly with the light intensity integrated over exposure time. A saturation curve can exist for each pixel, in which the greyscale dependence on exposure can be linear for small values of exposure, and can tend to an asymptotic value of 255 with increasing exposure. Noise can obscure the dependence for small values of the exposure. Accordingly, in step 110 of the method 100, pixel values within the ROI of the image can be linearized according to the saturation curve.

[0065] Next, calibration can be performed in step 110 of the method 100 by examining a set of images of one fuel bundle in one fixed position and orientation, taken over a range of gain settings and exposure times. For each gain setting, a least squares fit can be used to fit a function of the greyscale to exposure time correspondence for the set of images. The result can be a calibration scaling function, which is dependent on gain, exposure and greyscale pixel value, that can then be used to convert the linearized greyscale image into a calibrated image with an objective intensity by transforming the greyscale value for each pixel to a calibrated value for the given shutter speed and gain factor, valid up to a multiplicative constant. The constant can be the same for all the images in a set of images. The result for the image is that each pixel contains a calibrated value that is not constrained to be between 0 and 255. This allows comparison of images taken with different exposures and gain settings.

[0066] For example, referring to FIG. 5B, a relationship is shown derived by analyzing multiple images of the same object taken in the same position with a range of exposure times and gain settings. Using this relationship, pixel values can be adjusted to calibrated values.

[0067] In step 112 of the method 100, a mask can be applied to the image to isolate a section of the region of interest of the image. Application of the mask can begin by determining the direction in which the fuel bundle is tilted. In this example, which is dependent upon the end structure of the fuel bundle 26 as shown in FIG. 2B, to establish a tilt angle, the position of at least seven of the eighteen pin centers in the outer ring can be identified in order to trace the elliptical shape of the outer ring. For example, as shown in FIG. 6A, an operator can manually select the pin centers of the fuel bundle 26 in the image by adjusting the position of a selection tool 66 through a user interface 68. Once the ellipse associated with the outer ring is determined, a mask can be created by selecting all pixels within the ROI having a calibrated intensity of greater than a predetermined amount of the maximum calibrated intensity for the image. The masked fuel bundle 26a is shown in FIG. 6B, and in this case the predetermined amount is 20%. The masked fuel bundle 26a includes the crescent of Cerenkov radiation glow 58 and the Cerenkov radiation glow 72 between the pins.

[0068] Referring now to FIG. 7A, for the purposes of a mask used in determining the external integral, as described herein, the image can be truncated to select only those pixels between parallel lines 70 that are tangential to the endplate ellipse, and on the side to which the fuel bundle is tilting. The mask can be further refined to eliminate the fuel bundle and spaces within it, based on the endplate geometry and fuel pin arrangement. The externally masked fuel bundle 26b, as shown in FIG. 7A, which includes only the crescent of Cerenkov radiation glow 58, but extraneous artifacts, such as reflections from other items, are eliminated because only a specific portion of the image is considered.

[0069] For the purposes of a mask used in determining the internal integral, as described herein, a mask can be applied to eliminate all but the light between the outer rings and the first intermediate ring. The internally masked fuel bundle 26c is shown in FIG. 7B, which includes only the Cerenkov radiation glow 72 between the pins. This mask can be based on the geometry of the endplate and fuel pin arrangement, and can be constructed, at least in part, by dimensions and positions of the internal pins, either inputted by an operator by adjusting the position of a selection tool 66 through the user interface 68, as shown in FIG. 8A, or identified automatically by processing software carrying out the image analysis 104.

[0070] Step 114 of the method 100 consists of summing the pixel values for the masked image to yield an intensity value. In this example, which again is dependent upon the end structure of the fuel bundle as shown in FIG. 2B, two integrated light levels can be calculated. The first is the integral of the Cerenkov radiation produced in an external, selected region of the fuel bundle, which is referred to as the external integral. The region is defined to improve the signal to noise ratio and eliminate extraneous reflections, objects and other items that could affect the results. The second integrated light level is the integral of the Cerenkov radiation produced in an internal, annular region between the outermost two rings of pins in the bundle, which is referred to as the internal integral. The external integral can provide a total external intensity value for the image that can be compared with the corresponding intensity value of other images, and can be preferred over the internal integral because it is generally independent of the tilt angle of the fuel bundle. Calculating an external integral, an integral, or a combined external and internal integral can yield an intensity value for the image that can be correlated to the irradiation and cooling histories of the fuel bundle.

[0071] With reference again to FIGS. 1A and 2A, the internal integral can have a strong dependence on tilt angle, which can be defined as the angle between the optical axis 19 of the viewing device 10 and the fuel bundle longitudinal axis 30, because the amount of the Cerenkov radiation obscured by the fuel pins 28 increases with the tilt angle. Unless the tilt angle is zero, the fuel pins 28 can obscure part of the Cerenkov radiation between the fuel pins. When measuring the external integral, only light from the half of the bundle that is fully visible (not obscured by the fuel bundle itself) is measured (see FIG. 7A), and hence tilt angle is not a consideration.

[0072] The internal integral can be calculated by first calculating the angle at which the bundle is tilted. This can be a geometric calculation that can be carried out, for example, by comparing the position of the centroid of the region having an intensity greater than 20% of the maximum intensity in the image to the position of the center of the fuel bundle endplate. Referring to FIG. 8B, Cerenkov radiation travels in a direction 34 from the fuel bundle 26 to a viewing device (not shown). A visible fraction 38 of a volume 36 between the outer and intermediate rings of fuel pins 28 can be recognized and used to correct for the tilt angle. The correction assumes that the Cerenkov radiation is angularly isotropic (i.e. its emission intensity it is not dependent on its direction), uniformly distributed in the volume 36 between the rings of the fuel pins 28, and that the length of the fuel bundle 26 is small compared to the distance between the bundle and the observer.

[0073] For images with lower quality (e.g., taken at low exposure, with extraneous items in the field of view), steps in the analysis 104 of the method 100 can yield improved results. For example, if a fuel bundle is relatively difficult to see in an image, brightness and contrast of the image can be enhanced. Further, as described herein, the image can be examined for anomalies that can affect the ability to take all of the pixels in the image that contain useful information and could interfere with measuring the light intensity, and external items that do not include the Cerenkov radiation glow can be removed. As described herein, through a user interface, an operator can manually select a spurious feature for cropping to refine the ROI. Pixel brightness for the selected, cropped area can be set to black, below the threshold for the mask, ensuring that the extraneous bright areas are not included in calculating the external integral. Following this, the raw greyscale image can then be converted to a calibrated image, one or more masks can be generated, and the total light intensity in the masked region(s) of the image can be calculated, as described herein.

[0074] By way of illustration regarding the methods described herein, and referring back to FIG. 1A, using the device 10, in which the lens 12 consisted of a f/2.8 250 mm lens, and the camera device 18 consisted of a NIKON™ COOLPIX 5000™ digital camera, the inventors imaged five CANDU-type natural uranium bundles. The characteristics of the five CANDU-type fuel bundles are given in Table 1. The bundles were imaged in the end-on position, at an underwater location at a 15 foot water depth in a clear area of the storage bay floor, with the device 10 either mounted on a fixed tripod, or hand-held. Some of the images of the dimmest bundle, taken with underwater bay lights on, were not found to contain any discernable information. The remaining images were analyzed in accordance with the methods described herein.

Bundle	Fuel Type [Endplate type]	Total Burnup (MWd/kgU)	Cooling Time of Fuel Bundle (days)	Estimated Decay Heat (Watts)
A	36-element Natural UO_2 [ANB Bruce]	10.3	176	84.8
B	36-element Natural UO_2 [CANDU 6]	9.6	352	17.8
C	36-element Natural UO_2 [ANB Bruce]	10.9	352	13.9
D	36-element Natural UO_2 [ANB Bruce]	8.9	1781	4.38
E	36-element Natural UO_2 [ANB Bruce]	4.0	6868	1.96

Table 1. Imaged CANDU-type nuclear fuel bundles.

[0075] As described herein, images were analyzed to yield two measures of Cerenkov radiation intensity: the external integrated intensity; and the internal integrated intensity. FIG. 9A shows results of external integrated intensity values from the images, calculated according to the methods described herein. Similarly, FIG. 9B shows the internal integrated intensity values. FIGS. 9A and 9B demonstrate that the measured intensity of Cerenkov radiation can be correlated approximately to the calculated decay heats of the bundles.

[0076] It should be appreciated that decay heat and Cerenkov radiation are both caused by the decay of radioactive nuclides produced by fission. Decay heat can be defined generally as the sum total of all the radioactive decay energy in the fuel (minus the energy carried away by neutrinos), whereas Cerenkov radiation is produced by high-energy electromagnetic radiation that escapes from the fuel pins. Therefore, the contribution of specific radionuclides, each of which can produce different types and amounts of energy per decay and can have different radioactive decay rates, to decay heat and to Cerenkov radiation can be different.

[0077] Cerenkov radiation (in water) is the result of electrons with velocities greater than the speed of light in water. The minimum kinetic energy of such electrons is approximately 0.262 MeV. All electrons with energy greater than this minimum or threshold energy produce Cerenkov radiation as they travel in water. As the electrons lose energy by ionization and scattering, they slow down, and stop producing Cerenkov radiation when their kinetic energy drops below the threshold energy. The total number of Cerenkov photons produced by a high-energy electron is essentially proportional to its total path-length in water before it drops below the threshold energy. The rate of Cerenkov photon production in water is roughly 200 photons of 400 nm wavelength per cm of electron path length, where 1 cm path length corresponds approximately to a 2 MeV electron.

[0078] Certain radionuclides produce energetic electrons directly by β-decay. Gamma radiation from radioactive decay can also give rise to Cerenkov radiation because energetic gamma rays can produce electrons and positrons with energies above the Cerenkov threshold. Gamma-rays give rise to energetic electrons by Compton scattering from atomic electrons in the fuel, fuel pins, and in water. For example, the minimum gamma-ray energy required to produce an electron with 0.26 MeV is 0.51 MeV. Gamma-rays with energies above 1.022 MeV can directly produce electrons and positrons by pair production.

[0079] These sources of energetic electrons in the vicinity of irradiated fuel pins can be generally classified into three categories: (i) electrons produced by β-decay inside the fuel, with enough energy to exit the fuel pin (since the range of electrons is limited, the sources of such external electrons are necessarily relatively close to the surface of the fuel and do not penetrate the cladding); (ii) electrons produced by γ-ray interactions in the fuel pin material itself (while the primary γ-rays can originate from deep inside the fuel, the sources for the secondary electrons that escape the fuel must again be close to the surface of the fuel and do not penetrate the cladding); and (iii) electrons produced by γ-rays that exit the fuel pin and interact directly in the water surrounding the fuel pin.

[0080] These three categories of Cerenkov radiation producing mechanisms can emanate in differing proportions from the fuel pins depending on the type and energy of the primary radiation and the geometrical details (shape and density distribution) of the fuel pins. Integrating these contributions over the energies of β-rays and γ-rays and the geometry of the fuel bundle, for a given radionuclide distribution, and characteristic of a given burn-up/cooling time history, can be carried out by probabilistic particle tracking computer codes, such as the Monte-Carlo N-Particle code.

[0081] However, in accordance with the methods described herein, the inventors have determined the relative Cerenkov radiation intensities for five fuel bundles with assumed identical geometry, and well-documented, diverse burn-up/cooling time histories. If it is assumed that the Cerenkov intensity is dominantly produced by the decay of a few (for example, 3 or 4) radionuclides with widely different half-lives, then the five data-points allow the extraction of relative contributions of each of the isotopes. The assumption of widely different half-lives can allow a reasonable fit over the wide range of burn-up/cooling time histories and also can ensure numerical stability.

[0082] It can be assumed that the Cerenkov radiation from long-cooled spent fuel bundles is dominated by the decay of ^{137}Cs, and ^{134}Cs. For short-cooled bundles, there may be contributions from ^{106}Rh, ^{144}Pr, and other radionuclides with even shorter radioactive half-lives. The decay characteristics of these four radionuclides are summarized in Table 2. The last row of Table 2 lists a hypothetical short-lived nuclide, X, with a half-life of 1/3 year or 4 months. As described below, this single short-lived nuclide can best represent the many short-lived radionuclides that contribute to the Cerenkov glow of fuel bundles that have cooled for a short time (i.e., cooling time of the order of 1 year or less).

Nuclide	Average fission yield from ^{233}U, ^{235}U, and ^{239}Pu (%)	Half-life (yr)	Average electromagnetic energy per decay (MeV)	Dominant radiation type
^{137}Cs	6.7	30.0	0.566	γ, β
^{134}Cs	7.7	2.06	1.555	γ
^{106}Rh	2.5	1.02	2.882	γ
^{144}Pr	5.0	0.780	1.2	β
X	5.0	0.33	N/A	N/A

Table 2. Radionuclides that dominate Cerenkov radiation production in spent fuel.

[0083] Given the power history of the fuel bundle, $P(t)$, the relative activity, A_i, of a particular radionuclide labeled by index i, can be estimated at any given time, t, from the following integral:

$$A_i(t) = \frac{f_i}{\tau_i} \int_{-\infty}^{t} P(t') e^{\frac{(t'-t)}{\tau_i}} dt' \qquad (1),$$

where f_i is the fractional yield per fission, i.e., the fission yield, and τ_i is the mean life of radionuclide i. If the Cerenkov radiation yield from radionuclide i is taken to be c_i, then the total relative Cerenkov radiation emission is given by:

$$C = \sum_i c_i A_i \qquad (2).$$

[0084] The inventors have experimentally obtained five different values of relative Cerenkov radiation yield for the fuel bundles, where the relative activities, A_i can be estimated independently for each bundle. The relative Cerenkov yield weighting factors, c_i, can be extracted for up to four different radionuclides by simultaneously solving the five equations obtained by applying Equation (2) to each bundle. Alternatively, the simultaneous equations can be solved by iteratively fitting the c_i values to minimize the total square error between the measurements and the fitted values of the relative Cerenkov yields.

[0085] The integral of Equation (1) can be numerically evaluated as follows. The entire history of the fuel bundle can be broken up into smaller periods of time, during each of which the fission power, i.e., the production rate of the radionuclide, is assumed to be constant. If the time of measurement is taken as the origin, i.e., $t = 0$, then for each period of non-zero power, P_n lasting from $-t_{n+1}$ to $-t_n$, the contribution to the integral is

$$\frac{f \cdot P_n}{\tau}\left(e^{-\frac{|t_n|}{\tau}} - e^{-\frac{|t_{n+1}|}{\tau}}\right) \qquad (3).$$

All the contributions until $t = 0$ are summed to give the total activity.

[0086] It was calculated that the ratio between the measured intensities of bundles D and E will be dominated by the relative contributions to Cerenkov radiation emission from the two long-lived nuclides only, ^{134}Cs ($t_{1/2}$ = 2.06 y) and ^{137}Cs ($t_{1/2}$ = 30.0 y). If only these two radionuclides contributed to Cerenkov glow, then the measured intensity of these two bundles, along with the measured intensity of any one of the other three bundles (for normalization) can be used to deduce the relative contributions of ^{134}Cs and ^{137}Cs. Therefore, the relative intensities of the three brightest bundles, A, B and C, provide both the overall normalization, and the contribution due to one or two other nuclides of half-life shorter than two years. The inventors determined that the best overall fit can be obtained by a single nuclide, of half-life somewhat shorter than either ^{106}Rh or ^{144}Pr; nuclide X in Table 2 represents this hypothetical nuclide.

[0087] For the fitting procedure, only values of the external integrated intensity, obtained from images taken at an image intensifier maximum gain setting were used. For each bundle, the average value from all such images was used as the best experimental estimate of Cerenkov radiation emission, and the standard deviation was used as the estimated experimental uncertainty.

[0088] Table 3 provides the experimentally measured and fitted external integrated intensities from the above procedure. Table 4 gives some details of the individual nuclide activities calculated from the irradiation histories, and the fitted relative contribution of each nuclide to the total measured intensity.

Bundle	Measured Intensity	1-σ Experimental Uncertainty	1-σ Experimental Uncertainty (%)	Best-Fit Intensity	(Best-Fit - Experimental)/(Best-Fit) Ratio (% deviation)
A	4.36E+05	3.46E+04	7.9	4.32E+05	-0.84
B	7.94E+04	9.73E+03	12.3	8.45E+04	6.01
C	6.51E+04	1.83E+04	28.2	5.14E+04	-26.49
D	8.19E+03	1.23E+03	15.0	7.78E+03	-5.29
E	1.82E+03	7.84E+01	4.3	1.82E+03	0.18

Table 3. Measured and fitted external integrated intensities.

Bundle	Calculated nuclide activity relative to ^{137}Cs in bundle E			Fitted Cerenkov radiation contribution relative to ^{137}Cs in bundle E		
	X	^{134}Cs	^{137}Cs	X	^{134}Cs	^{137}Cs
A	0.15277	2.13829	3.77980	194.56	55.17	3.78
B	0.02041	0.79415	3.04844	25.99	20.49	3.05
C	0.01555	0.29755	2.67871	19.81	7.68	2.68
D	0.00001	0.09342	2.14164	0.01	2.41	2.14
E	0.00000	0.00261	1.00000	0.00	0.07	1.00

Table 4. Nuclide activities calculated from irradiation history, and Cerenkov radiation contributions determined by fitting to measured intensities.

[0089] Finally, the overall relative weighting factors (c_i in Equation (2)) for the measured external integrated Cerenkov radiation intensities, due to the different nuclides were found to be:

$$X : {}^{134}Cs : {}^{137}Cs :: 1270 : 25.8 : 1 \qquad (4).$$

[0090] This fitted ratio is reasonable given the relative electromagnetic decay energies of ^{134}Cs and ^{137}Cs, assuming for X the general trend that shorter-lived radionuclides have correspondingly higher decay energies, and considering that the decay energy (i.e. the total energy of the products of radioactive decay) is doubly weighted for Cerenkov yield, in the sense that higher decay energy leads both to more β and γ radiation, i.e., Cerenkov radiation precursors escaping from the bundle and the generation of light in the water. Accordingly, the relative Cerenkov radiation yield for any bundle with arbitrary irradiation and storage history can be calculated, given the relative Cerenkov yield ratio of the contributing radionuclides as deduced in Equation (4).

[0091] To illustrate the sensitivity of the Cerenkov viewing device for typical fuel bundles, the relative Cerenkov radiation intensity for CANDU-type bundles with different burn-ups and cooling times is plotted in FIG. 10. For these curves, it is assumed that the bundle is irradiated continuously at a constant power for 667 days (1.82 years). This value was chosen to allow a clearer representation in the log scale. The power level is adjusted to give the desired burn-up. The activity of each of the three nuclides, X, ^{134}Cs, and ^{137}Cs, is followed during and after the irradiation. The Cerenkov radiation intensity is calculated using the relative weighting factors ratio of Equation (4). The units of relative intensity in FIG. 10 are the same as the external integrated intensity used for fitting the nuclide ratio described above.

[0092] A typical measurement point was shown to have a relative error bar of about 10%. The "detection limit" is based on using 10% of the intensity of the dimmest bundle imaged. The detection limit is assumed to be the point at which the absolute error is approximately equal to the value of the quantity being measured. The detection limit increases as the sensitivity of the measurement decreases. The detection limit will vary depending on the conditions under which a particular set of bundles is imaged. In particular, the detection limit will be higher than shown in FIG. 10, for example, if the fuel bundles are: (i) imaged at a depth of more than 15 feet under water; (ii) imaged with a smaller lens (e.g., 105 mm); or (iii) imaged under adverse conditions of ambient lighting and interfering reflectors, scatterers, sources, and UV absorption in the water. As well, accuracy of measurement is lower at low Cerenkov radiation levels, so the useful range over which measurements can be made may be limited by requirements for accuracy.

[0093] Further, it should be appreciated that the quantitative intensity measurements described herein, and the decay heat estimations based thereon, can be relative in the sense that they may depend on the conditions that exist when images of a fuel bundle are obtained. For example, water quality in the storage bay, quantum efficiency of the filters and sensors of the device used to view and obtain the images, and the optical path length from the fuel bundle to the device, are all conditions which may affect intensity measurements. Thus, it may be useful to position a source of Cerenkov radiation or UV light, whose intensity is known *a priori*, in the storage bay to serve as an objective comparator. For example, a radioactive source (e.g., Cobalt-60) of known strength, or a source of UV light having an intensity that is known or can be measured (and placed alongside the fuel bundle at the bottom of the storage bay, or positioned above the bay and directed downwardly to reflect UV light back to the bridge) can be implemented. The intensity of the known source can be compared to the intensity of Cerenkov radiation being emitted from the fuel bundle, to derive an objective intensity for the fuel bundle.

[0094] In summary, referring to FIG. 10, quantitative measurements were found to be consistent for fuel bundles with a wide range of burn-up and cooling times, ranging from 10 MWd/kgU burn-up and 6 months cooling time to 4 MWd/kgU burn-up and 19 years cooling time. These results can therefore be extrapolated to use for quantitative measurements for CANDU fuel bundles ranging from 20 MWd/kgU burn-up and 6 months cooling time to 2.5 MWd/kgU burn-up and 40 years cooling time.

[0095] Although CANDU-type fuel bundles in particular are described herein, it should be appreciated that the present teachings are not limited as such. The teachings described herein can be used to assess other nuclear fuel bundles, and other radioactive objects having a variety of structures and geometries. For example, the inventors contemplate using the teachings described herein to assess PWR-type (Pressurized Water Reactor) fuel bundles, BWR-type (Boiling Water Reactors), or VVER-type (Water-Water Energetic Reactor) nuclear fuel bundles. FIG. 11A shows Cerenkov radiation being emitted from a PWR-type fuel bundle. FIG. 11B shows Cerenkov radiation being emitted from a BWR-type fuel bundle. FIG. 11C shows Cerenkov radiation being emitted from a VVER-type fuel bundle. The methodology of the image analysis 104 described above can be adapted to quantitatively measure the intensity of Cerenkov radiation being emitted from these different structures, and utilize the intensity as a basis for estimation of the radioactive decay heat. For example, it is expected that masks suitably configured to the different fuel bundle configurations could be used, and these may comprise rectangular or square masks for isolating external and internal regions of the bundles.

[0096] Reference is now made to FIGS. 12A and 12B, which illustrate an example of a system 200 for viewing Cerenkov radiation being emitted from an object.

[0097] The system 200 includes a lens 212, which can be, for example, a 105 mm refractive or a 250 mm catadioptic lens (mirror-lens combination to capture and focus the Cerenkov radiation), both of which can be generally compatible with UV frequencies of light. The lens 212 can be coupled to a UV band-pass filter 214 that is configured to suppress ambient visible light. The filter 214 is configured to selectively pass wavelengths associated with Cerenkov radiation, to reduce the contribution of other sources of light when viewing the fuel bundles. For example, the filter 214 can have a pass-band of between 300 nm and 330 nm.

[0098] The system 200 includes a camera unit 240 that is coupled to the lens 212 and the UV filter 214. The camera unit 240 includes an image intensifier device 242 and an image sensor device 244. The image intensifier 242 can consist of a UV sensitive photocathode, a micro-channel plate and a phosphor viewing screen that amplifies the collected and focused UV light and presents an image in the visible spectrum. The image sensor device 244 can consist of a CCD, or an active pixel sensor, for example, a complementary metal-oxide-semiconductor (CMOS) sensor. The lens 212, the filter 214, the image intensifier device 242 and the image sensor device 244 can all be aligned along an optical axis.

[0099] In the camera unit 240, the image sensor device 244 can be mounted generally at an image plane of the image intensifier device 242, to receive and record images of the object via the lens 212 and the UV filter 214. This arrangement of the image sensor device 244 directly at the output of the image intensifier device 242 means that images of the object can be transmitted from the lens 212 to the image sensor device 244 generally in focus, and can render the use of one or more relay lenses unnecessary. In some particular examples, a PHOTONIS™ ICU™ device (intensified camera unit; for example, models PP03000AE, PP0300AP or variations thereof may be suitable) can be implemented as the camera unit 240.

[00100] The system 200 further includes a processor 246 coupled to the image sensor device 244 of the camera unit 240. The processor 246 is configured to receive an image signal from the image sensor device 244, with images of the object encoded therein. The image signal conveyed to the processor 246 can be a digital signal, and can be encoded, for example, using Serial Digital Interface protocol or Camera Link protocol.

[00101] The processor 246 can be configured to serve various functions. First, for example, the processor 246 can be configured to convert the image signal into a format that can be shown in a viewfinder of a display 248, providing a means for an operator to view images of the object, which can be either still images, or a "real time" view of the object, or both. In some examples, a viewfinder of the display 248 can be a digital viewfinder. In some particular examples, a LITEYE™ LE 600™ display can be implemented as the display 248.

[00102] Second, the processor 246 can be configured to convert the image signal into still images that can be further analyzed and/or stored into a memory 250, which can be, for example, a flash memory. Third, the processor 246 can be configured to receive input from the operator through a user input 252 to control the operation of the camera unit 240, among other things. The user input 252 can consist of, for example, a keypad or a touchscreen. Further, the processor 246 can be configured, with a suitable suite of software, to carry out the image analysis 104 functionality described above in relation to FIG. 3.

[00103] The system 200 can further include an accelerometer 254 coupled to the processor 246. The accelerometer 254 can be configured to detect motion of the system 200, and the processor 246 can be configured to compensate for any blurring of the object that is induced by the motion. The system 200 can yet further include an audio recorder 256 coupled to the processor 246, which can be configured to record an audio note associated with the images of the object as they are being obtained.

[00104] As seen in FIG. 12B, in some examples, the components of the system 200 can be integrated into a single device, which can be sized and shaped to be a handheld device. The system 200 can include at least one handle 258. The system 200 can be battery powered for portability and ease of use.

[00105] While the above description provides examples of one or more processes or apparatuses, it will be appreciated that other processes or apparatuses may be within the scope of the accompanying claims.

CLAIMS

We claim:

1. A method of viewing Cerenkov radiation being emitted from an object, comprising:

obtaining at least one image of the object; and

calculating an intensity value for at least a portion of the image.

2. The method of claim 1, further comprising, prior to the step of calculating, defining a region of interest within the image, and wherein the step of calculating comprises calculating an intensity value for the region of interest.

3. The method of claim 2, wherein the step of defining comprises cropping the image.

4. The method of claim 3, wherein an external area of the image relative to the object is cropped.

5. The method of claim 3 or 4, wherein an internal area of the image relative to the object is cropped.

6. The method of any one of claims 1 to 5, further comprising, prior to the step of calculating, examining the image and correcting for at least one of noise, underexposure and overexposure.

7. The method of any one of claims 1 to 6, further comprising, prior to the step of calculating, calibrating the image by adjusting pixel values.

8. The method of claim 7, wherein the pixel values are adjusted based on exposure time and gain settings used in the step of obtaining the image.

9. The method of any one of claims 1 to 8, wherein the step of calculating comprises summing pixel values for the portion of the image to yield the intensity value.

10. The method of claim 9, further comprising, prior to the step of calculating, applying a mask to isolate a section of the image.

11. The method of claim 10, wherein the step of applying comprises selecting pixels having an intensity of greater than a predetermined amount of a maximum intensity.

12. The method of claim 11, wherein the predetermined amount is about 20%.

13. The method of any one of claims 10 to 12, wherein the step of applying comprises selecting pixels within an external region of the object, and the step of calculating comprises summing pixel values for the external region.

14. The method of any one of claims 10 to 13, wherein the step of applying comprises selecting pixels within an internal region of the object, and the step of calculating comprises summing pixel values for the internal region.

15. The method of claim 14, wherein the step of applying comprises determining a tilt angle of the object relative to an optical axis, and correcting the intensity value based on the tilt angle.

16. The method of any one of claims 1 to 15, further comprising determining radioactivity of the object based on the intensity value.

17. The method of claim 16, wherein the step of determining comprises correlating a decay heat value for the object based on the intensity value.

18. The method of any one of claims 1 to 17, wherein the step of obtaining comprises receiving an image signal from an image sensor device.

19. The method of claim 18, wherein the step of obtaining comprises viewing the object through an image intensifier device coupled to the image sensor device.

20. The method of claim 19, further comprising, prior to the step of obtaining, mounting the image sensor device generally at an image plane of the image intensifier device.

21. The method of any one of claims 18 to 20, wherein the step of obtaining comprises storing a plurality of images of the object encoded in the image signal into a memory.

22. The method of any one of claims 18 to 21, wherein the step of obtaining comprises displaying images encoded in the image signal on a viewfinder.

23. The method of any one of claims 1 to 22, wherein the step of obtaining comprises viewing the object through a UV filter.

24. The method of any one of claims 1 to 23, wherein the object comprises at least one nuclear fuel bundle.

25. The method of any one of claims 1 to 23, wherein the object comprises at least one CANDU-type nuclear fuel bundle.

26. A system for viewing Cerenkov radiation being emitted from an object, comprising:

a lens;
a UV filter coupled to the lens;
an image intensifier device coupled to the UV filter; and
an image sensor device coupled to the image intensifier device.

27. The system of claim 26, wherein the image sensor device is mounted generally at an image plane of the image intensifier device.

28. The system of claim 26 or 27, wherein the image sensor device comprises a charge-coupled device (CCD).

29. The system of claim 26 or 27, wherein the image sensor device comprises an active pixel sensor.

30. The system of claim 29, wherein the image sensor device comprises a complementary metal-oxide-semiconductor (CMOS) sensor.

31. The system of any one of claims 26 to 30, wherein the UV filter is configured to selectively pass wavelengths associated with Cerenkov radiation.

32. The system of claim 31, wherein the UV filter has a pass-band of between about 300 nm and 330 nm.

33. The system of any one of claims 26 to 32, further comprising a processor coupled to the image sensor device, and configured to receive an image signal from the image sensor device.

34. The system of claim 33, further comprising a memory coupled to the processor, and configured to store a plurality of images of the object encoded in the image signal.

35. The system of claim 33 or 34, wherein the image signal is a digital signal.

36. The system of claim 35, wherein the digital signal is encoded using Serial Digital Interface protocol or Camera Link protocol.

37. The system of any one of claims 33 to 36, further comprising a viewfinder coupled to the processor, and configured to display images encoded in the image signal.

38. The system of any one of claims 33 to 37, further comprising an accelerometer coupled to the processor, and configured to detect motion of the system.

39. The system of claim 38, wherein the processor is configured to compensate for blurring of the object induced by the motion.

40. The system of any one of claims 33 to 39, further comprising an audio recorder coupled to the processor, and configured to record an audio note associated with an image encoded in the image signal.

41. The system of any one of claims 33 to 40, wherein the processor is configured to calculate an intensity value for at least a portion of an image encoded in the image signal.

42. The system of claim 41, wherein the processor is configured to crop the image to define a region of interest, and the intensity value is calculated for the region of interest.

43. The system of claim 42, wherein the processor is configured to examine the region of interest and correct for noise, underexposure or overexposure.

44. The system of claim 42 or 43, wherein the processor is configured to calibrate the region of interest within the image by adjusting pixel values based on exposure time and gain settings of the image sensor device.

45. The system of any one of claims 42 to 44, wherein the processor is configured to calculate the intensity value by summing pixel values for the region of interest within the image.

46. The system of any one of claims 42 to 45, wherein the processor is configured to apply a mask to isolate a section of the region of interest of the image.

47. The system of any one of claims 42 to 46, wherein the processor is configured to determine a tilt angle of the object relative to an optical axis, and correct the intensity value based on the tilt angle.

48. The system of any one of claims 26 to 47, wherein the image intensifier device and the image sensor device are integrated into a camera unit.

49. The system of claim 48, wherein the lens, the UV filter, the camera unit and the processor are integrated into a single device.

50. The system of claim 49, further comprising a viewfinder integrated into the single device.

51. The system of claim 49 or 50, wherein the single device is sized and shaped to be a handheld device.

52. The system of any one of claims 49 to 51, wherein the single device is battery powered.

53. A method of or a system for quantitative Cerenkov radiation viewing comprising any combination of one or more of the features described above and/or claimed above and/or illustrated in the drawings.

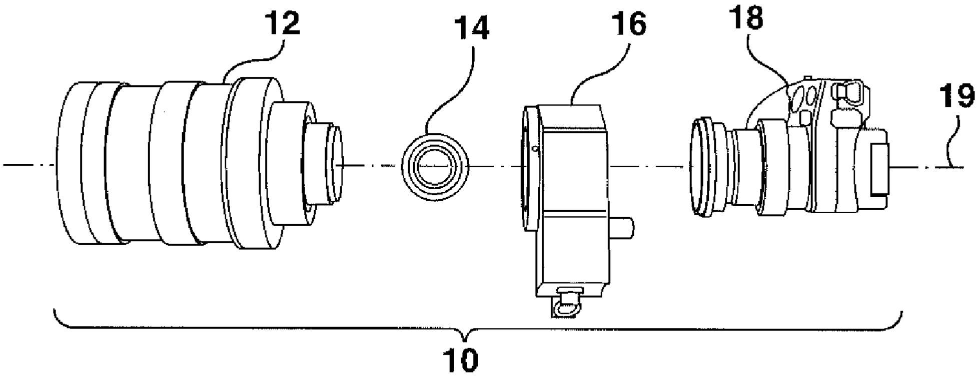

FIG. 1A

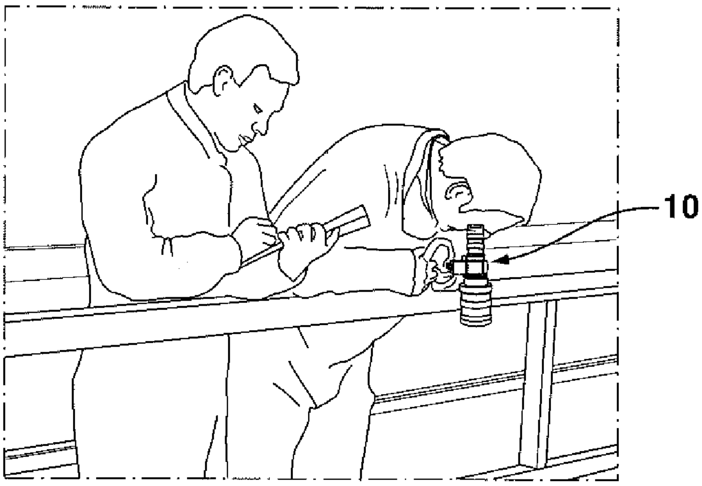

FIG. 1B

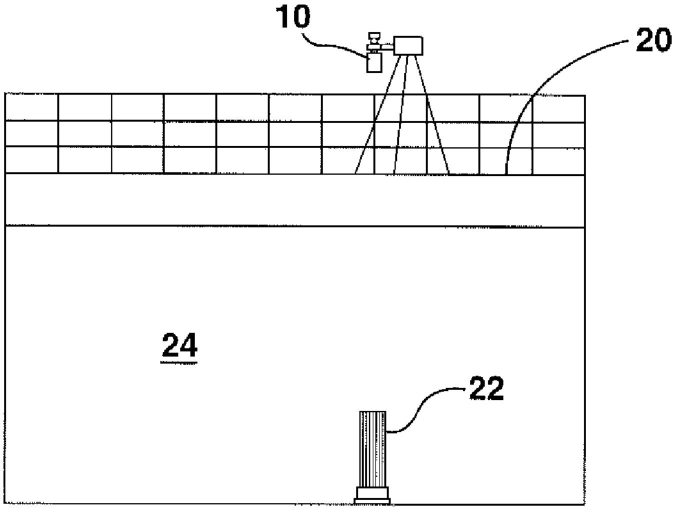

FIG. 1C

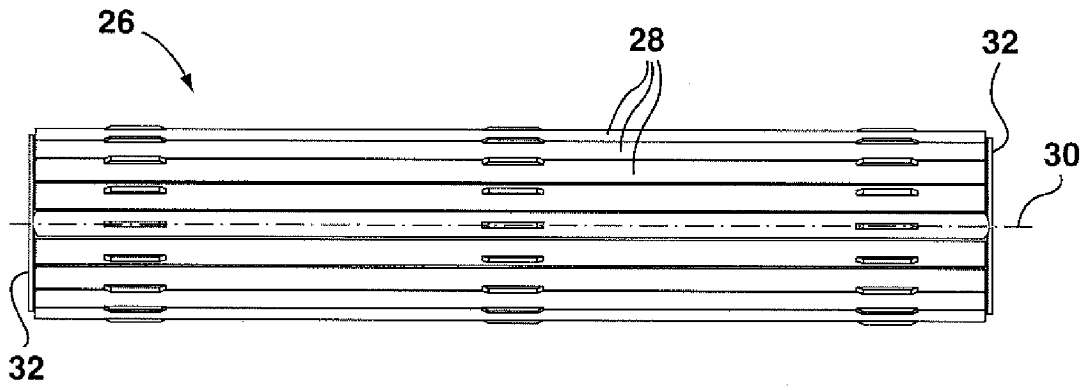

FIG. 2A

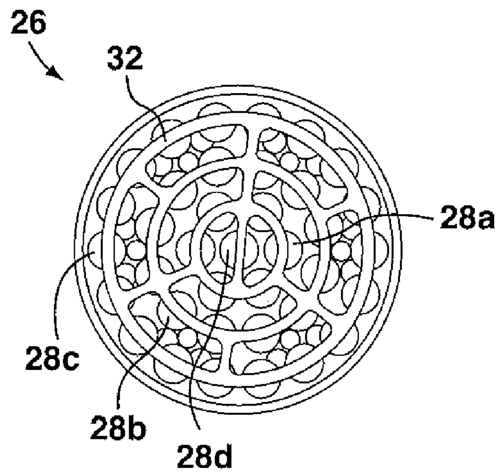

FIG. 2B

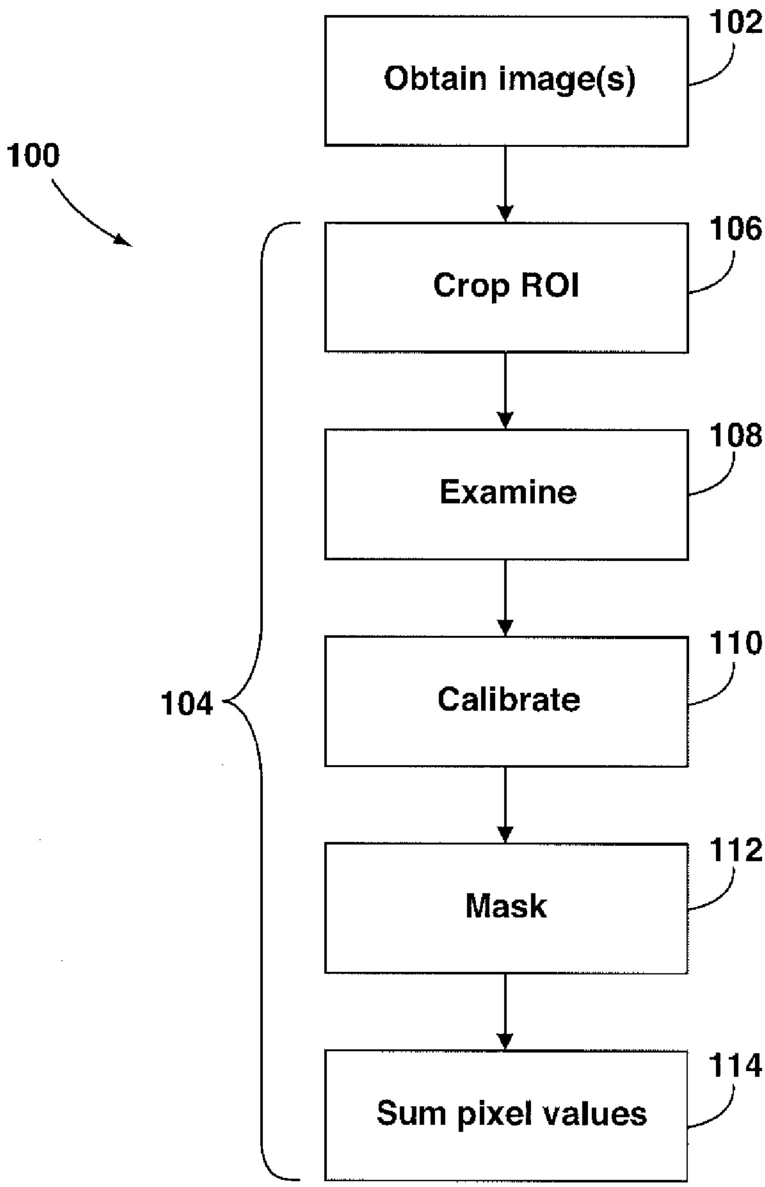
100
102
Obtain image(s)
104
106
Crop ROI
108
Examine
110
Calibrate
112
Mask
114
Sum pixel values

FIG. 3

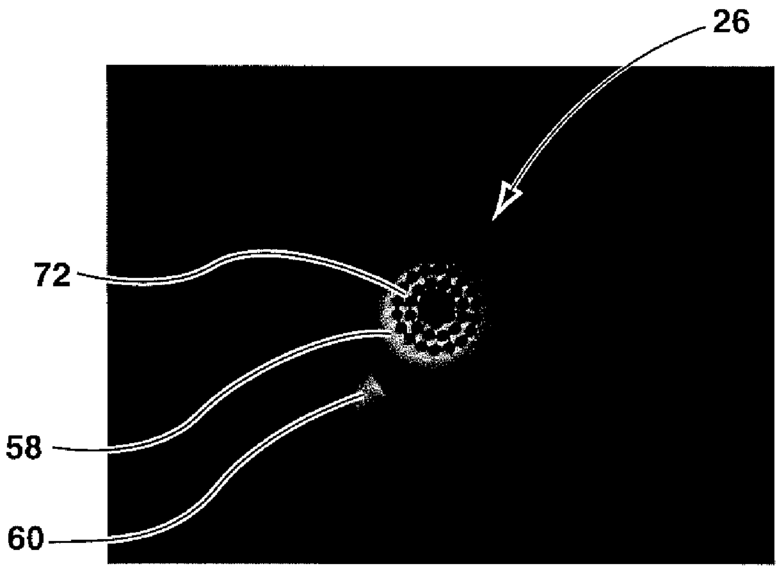

FIG. 4A

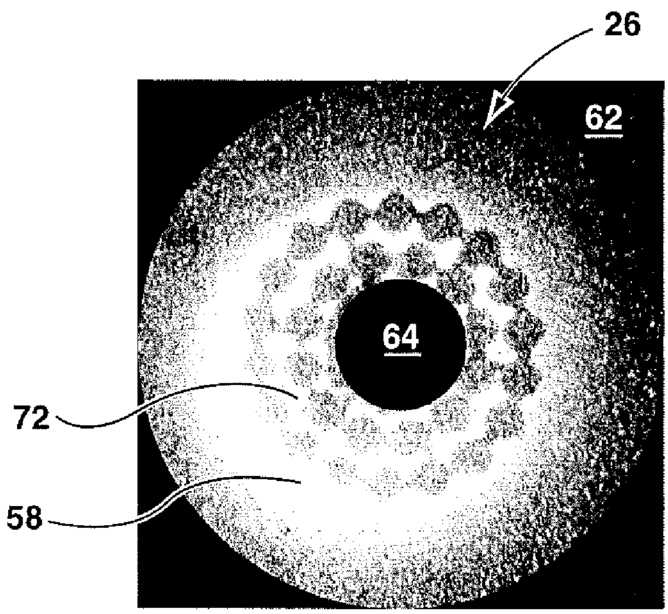

FIG. 4B

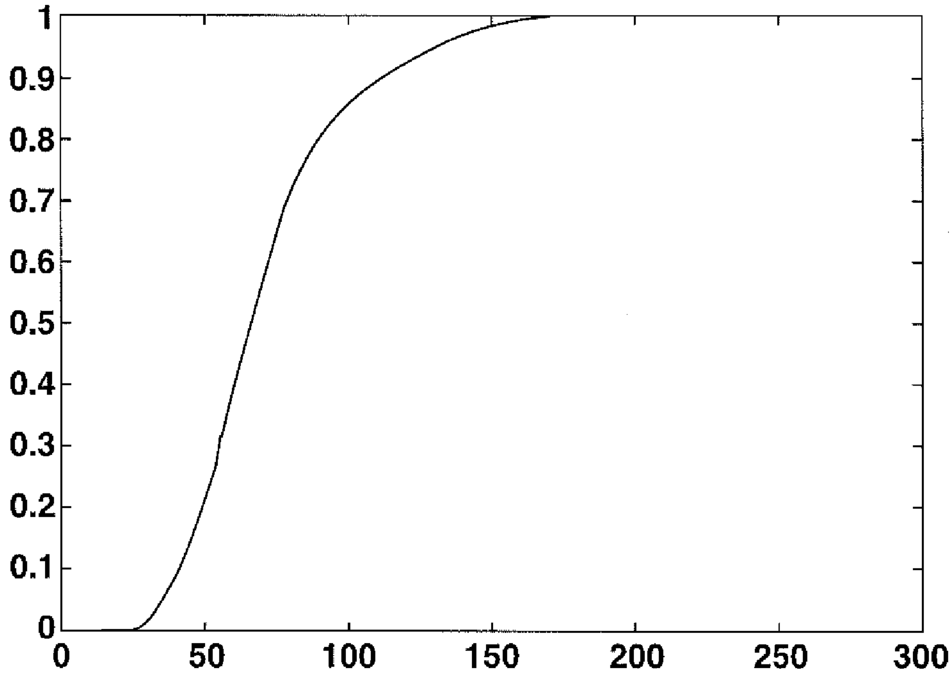
1
0.9
0.8
0.7
0.6
0.5
0.4
0.3
0.2
0.1
0
0
50
100
150
200
250
300

FIG. 5A

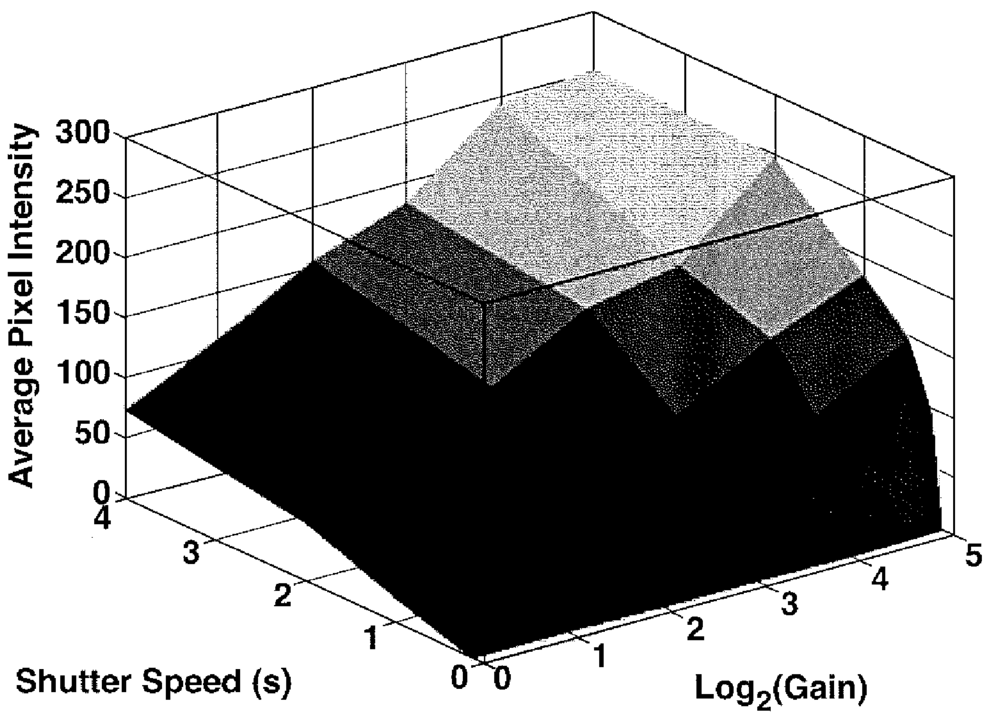
Average Pixel Intensity
300
250
200
150
100
50
0
4
3
2
1
0
Shutter Speed (s)
0
1
2
3
4
5
Log2(Gain)

FIG. 5B

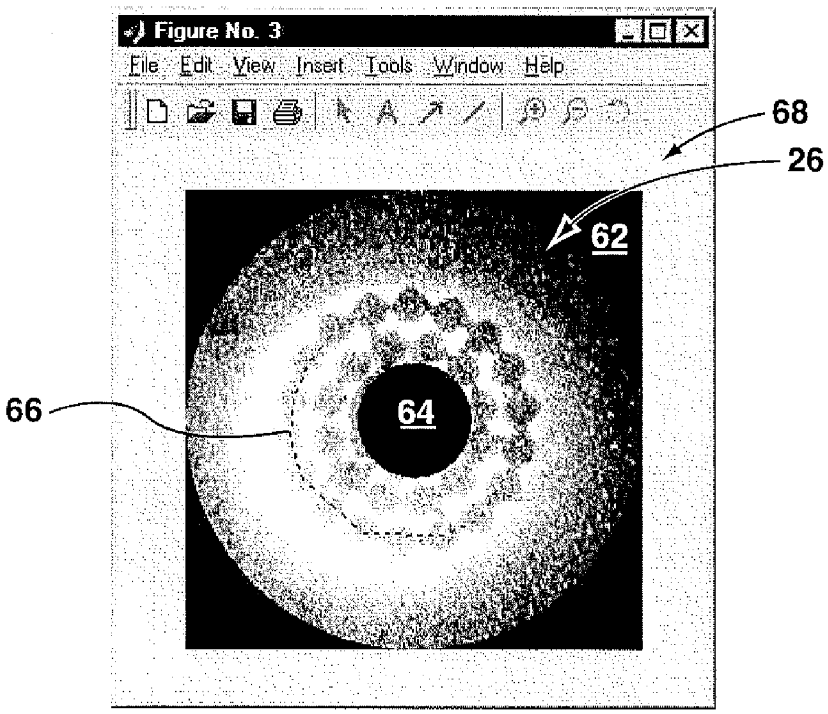
Figure No. 3
File Edit View Insert Tools Window Help
68
26
62
64
66

FIG. 6A

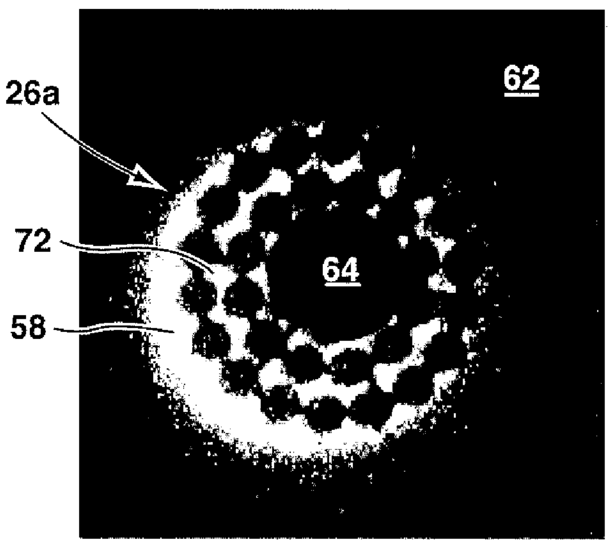
62
26a
72
64
58

FIG. 6B

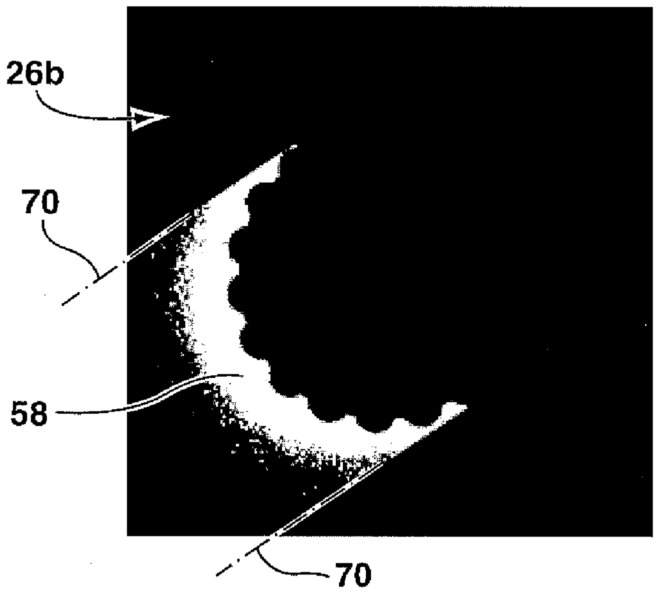

FIG. 7A

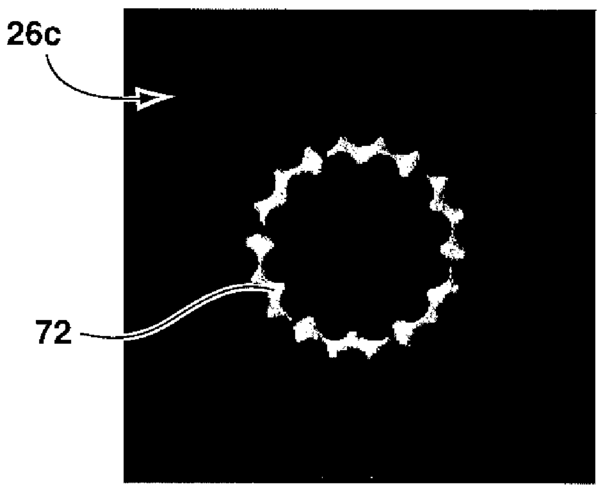

FIG. 7B

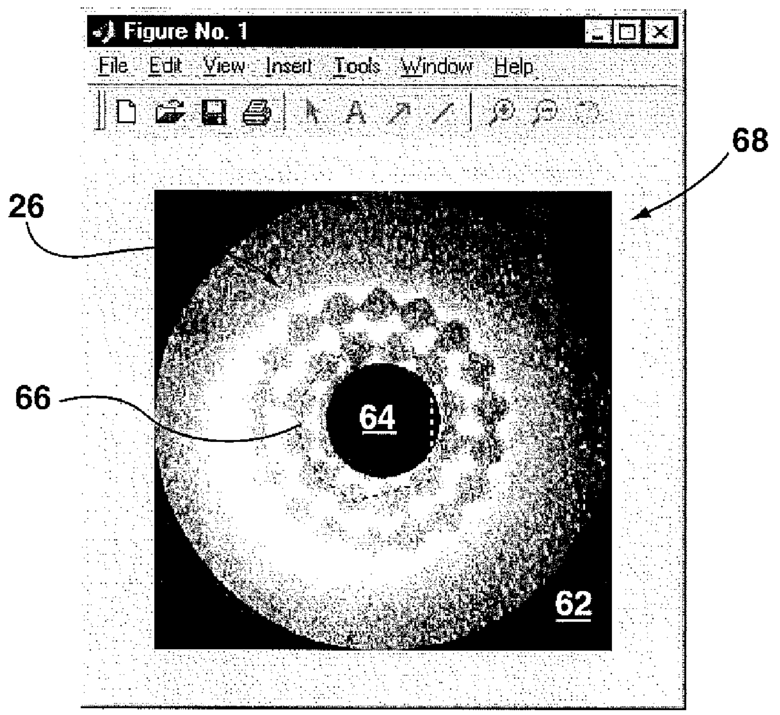
Figure No. 1
File Edit View Insert Tools Window Help
68
26
66
64
62

FIG. 8A

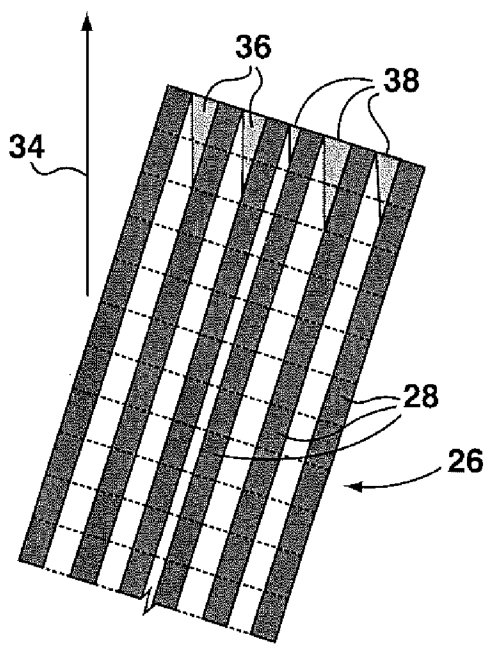
36
38
34
28
26

FIG. 8B

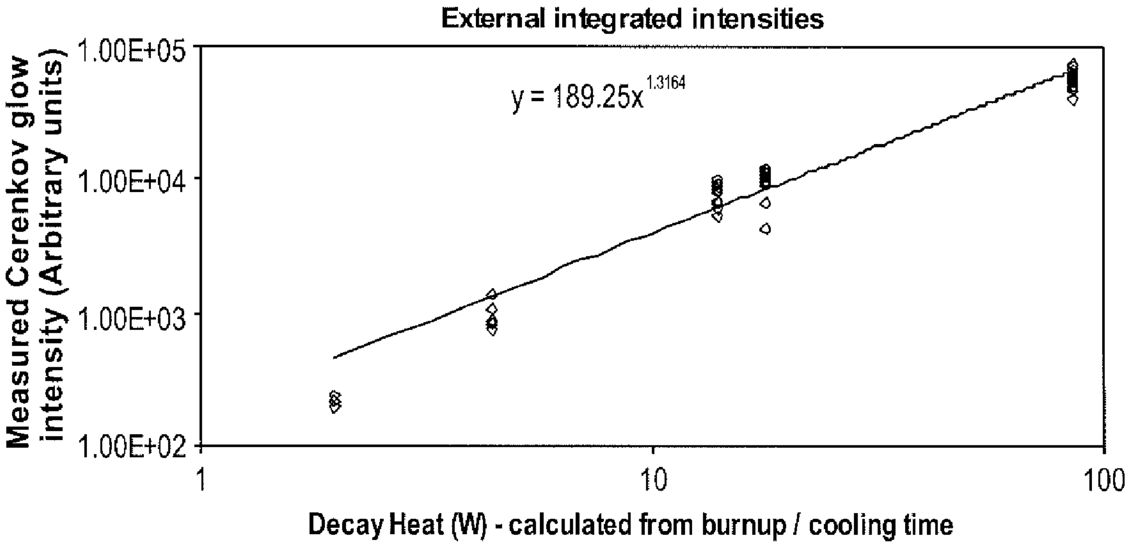
External integrated intensities
y = 189.25x^1.3164
Measured Cerenkov glow intensity (Arbitrary units)
1.00E+05
1.00E+04
1.00E+03
1.00E+02
1
10
100
Decay Heat (W) - calculated from burnup / cooling time

FIG. 9A

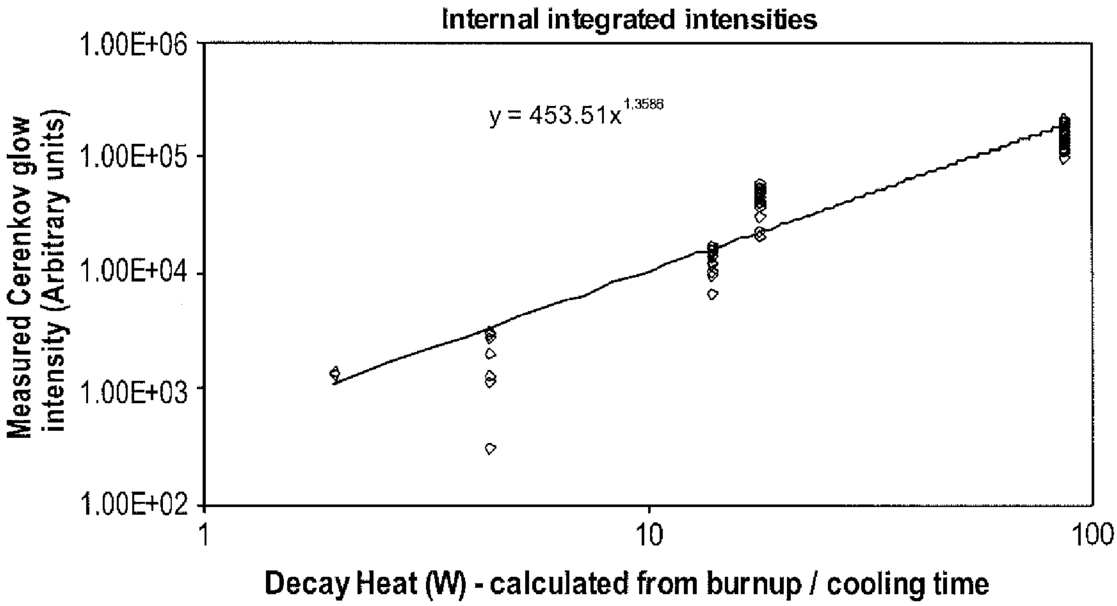
Internal integrated intensities
y = 453.51x^1.3586
Measured Cerenkov glow intensity (Arbitrary units)
1.00E+06
1.00E+05
1.00E+04
1.00E+03
1.00E+02
1
10
100
Decay Heat (W) - calculated from burnup / cooling time

FIG. 9B

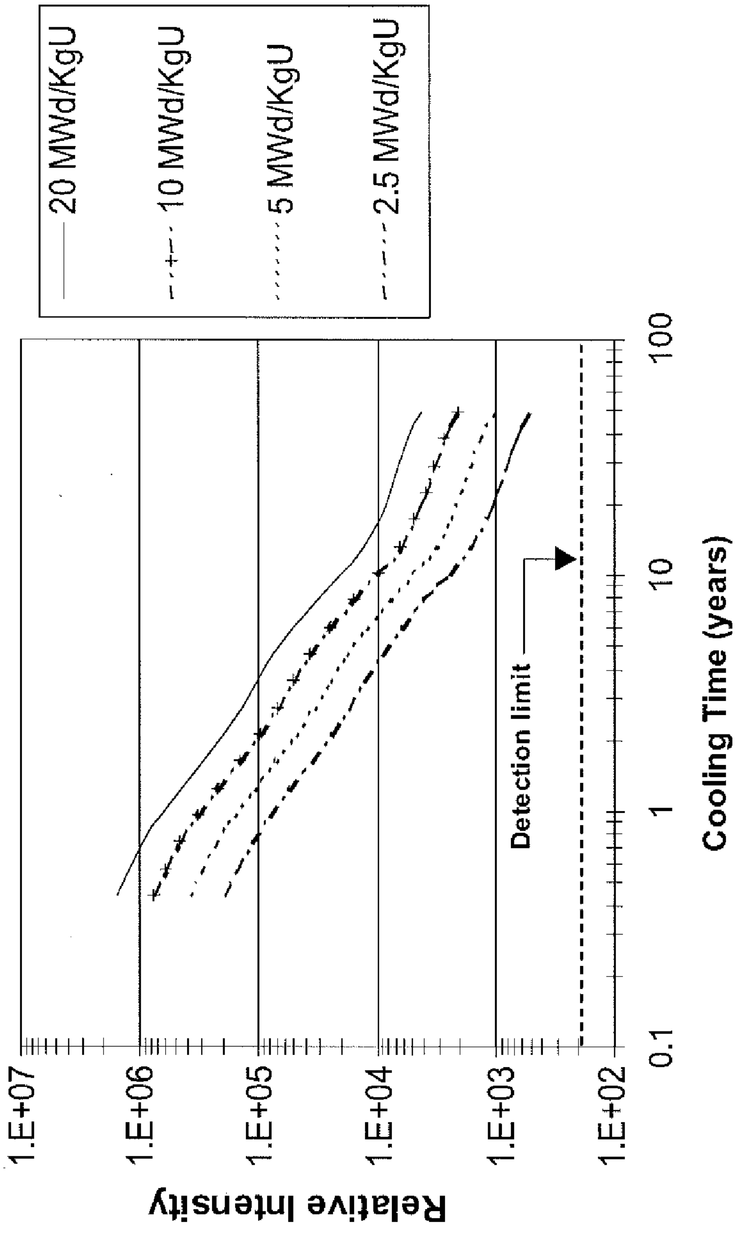
20 MWd/KgU
10 MWd/KgU
5 MWd/KgU
2.5 MWd/KgU
Relative Intensity
1.E+07
1.E+06
1.E+05
1.E+04
1.E+03
1.E+02
0.1
1
10
100
Detection limit
Cooling Time (years)

FIG. 10

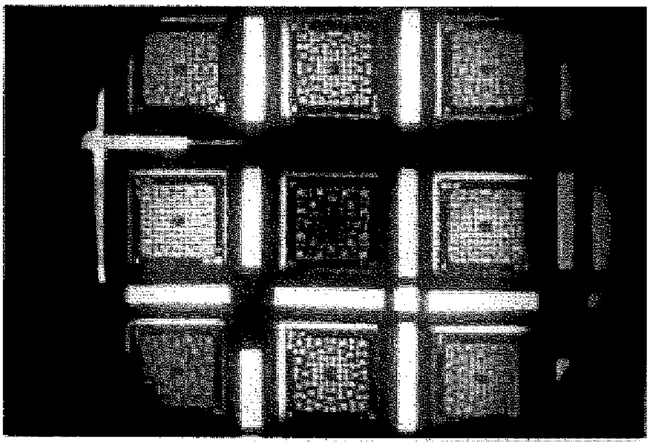

FIG. 11A

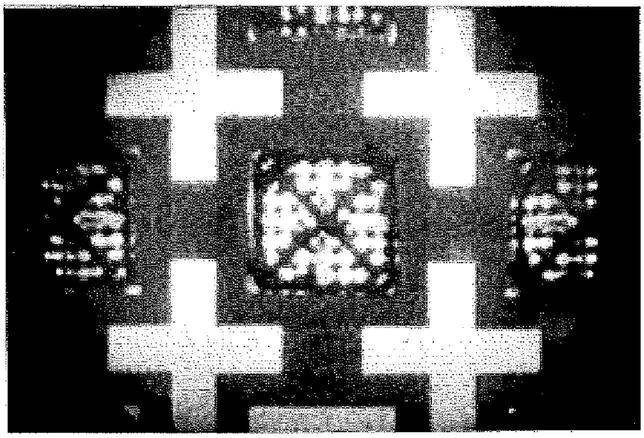

FIG. 11B

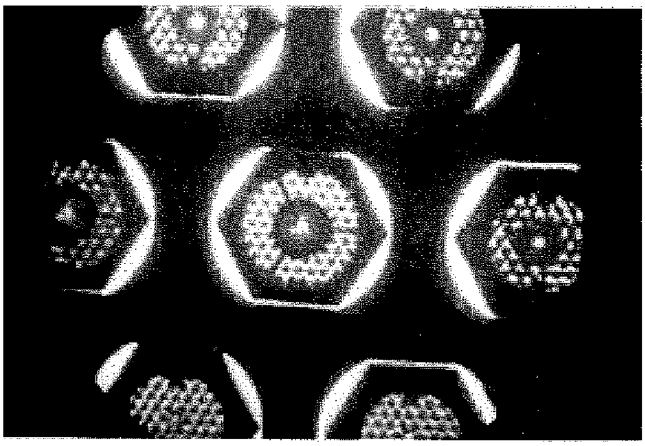

FIG. 11C

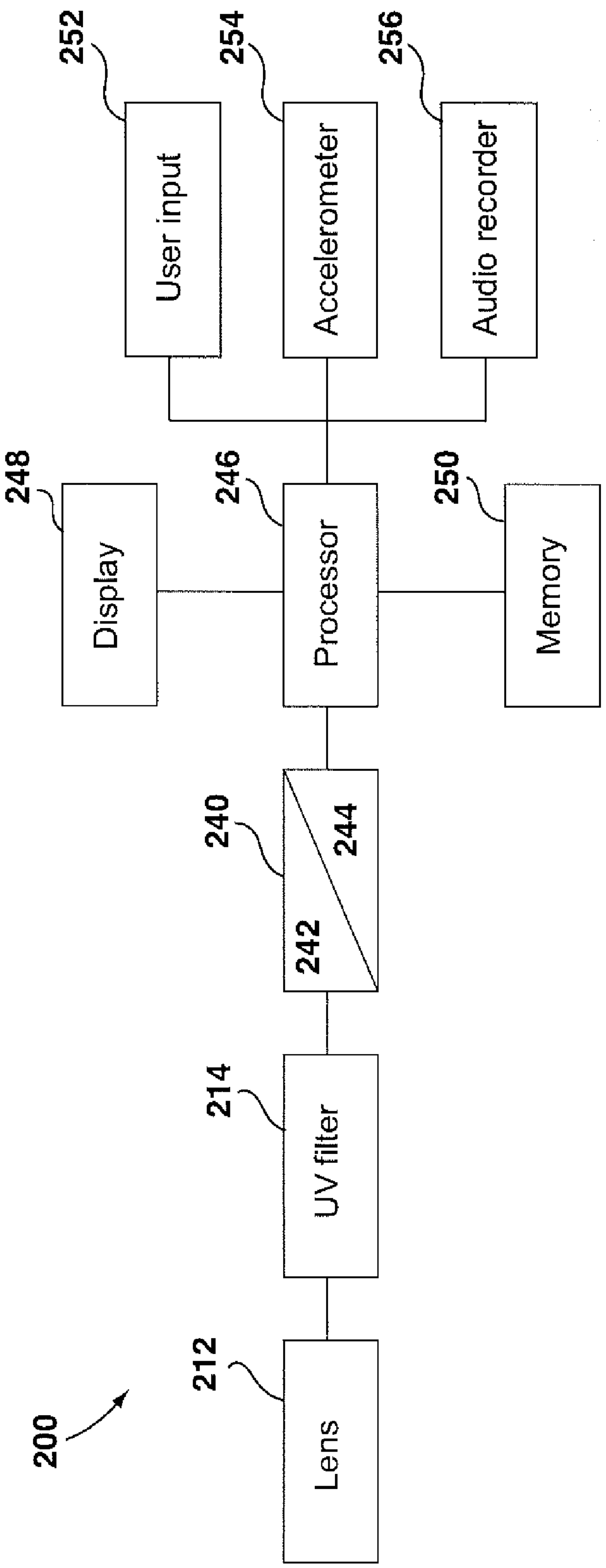
200
Lens
212
UV filter
214
240
242
244
Processor
246
Display
248
Memory
250
User input
252
Accelerometer
254
Audio recorder
256

FIG. 12A

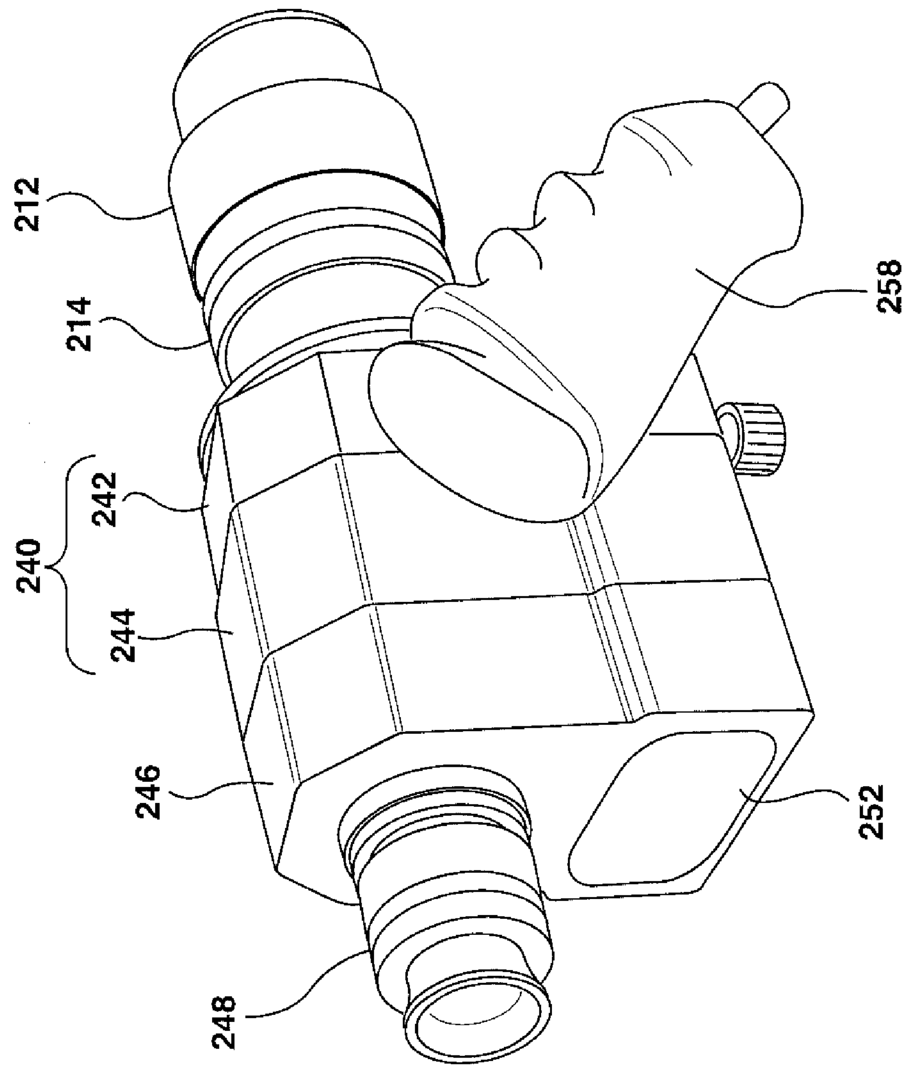

FIG. 12B

A. CLASSIFICATION OF SUBJECT MATTER
IPC: ***G01T 1/22*** (2006.01) , ***G01T 1/167*** (2006.01) , ***G01T 1/29*** (2006.01) , ***G21C 17/06*** (2006.01)
According to International Patent Classification (IPC) or to both national classification and IPC

B. FIELDS SEARCHED

Minimum documentation searched (classification system followed by classification symbols)
IPC: ***G01T 1/22*** (2006.01) , ***G01T 1/167*** (2006.01) , ***G01T 1/29*** (2006.01) , ***G21C 17/06*** (2006.01)

Documentation searched other than minimum documentation to the extent that such documents are included in the fields searched

Electronic database(s) consulted during the international search (name of database(s) and, where practicable, search terms used)
EPOQUE, TotalPatent, Canadian Patent Database (Intellect) and the World Wide Web. Keywords: cerenkov/cherenkov, UV filter, lens, sensor, mask, pixel, intensity, intensifier, CANDU

C. DOCUMENTS CONSIDERED TO BE RELEVANT

Category*	Citation of document, with indication, where appropriate, of the relevant passages	Relevant to claim No.
X Y	EP 1 112 459 (Elstien et al.) 4 July 2001 (04-07-2001) *See: [0030], [0034], [0038], [0041], [0047], [0051], [0052], [0074] and fig. 4.	1-9, 15-23, 26-45 and 47-52 10-14, 24, 25 and 46
Y	Castellano et al. "A multiresolution noise-removal algorithm for visual pattern recognition in imaging detectors", Computer Physics Communications, Vol. 66, Iss. 2-3, Oct. 1991 (10-1991), pgs. 293-307 *See: pg. 294-295: left-hand-column, last para; and section 2.1	10-14 and 46
Y	Attas et al. "A Cherenkov viewing device for used-fuel verification", Nuclear Instruments and Methods in Physics Research, Vol. 299, 20 Dec. 1990 (20-12-1990), pgs. 88-93 *See: Abstract	24 and 25

[ ] Further documents are listed in the continuation of Box C. [X] See patent family annex.

* Special categories of cited documents :

"A" document defining the general state of the art which is not considered to be of particular relevance

"E" earlier application or patent but published on or after the international filing date

"L" document which may throw doubts on priority claim(s) or which is cited to establish the publication date of another citation or other special reason (as specified)

"O" document referring to an oral disclosure, use, exhibition or other means

"P" document published prior to the international filing date but later than the priority date claimed

"T" later document published after the international filing date or priority date and not in conflict with the application but cited to understand the principle or theory underlying the invention

"X" document of particular relevance; the claimed invention cannot be considered novel or cannot be considered to involve an inventive step when the document is taken alone

"Y" document of particular relevance; the claimed invention cannot be considered to involve an inventive step when the document is combined with one or more other such documents, such combination being obvious to a person skilled in the art

"&" document member of the same patent family

Date of the actual completion of the international search	Date of mailing of the international search report
14 June 2012 (14-06-2012)	18 July 2012 (18-07-2012)

Name and mailing address of the ISA/CA
Canadian Intellectual Property Office
Place du Portage I, C114 - 1st Floor, Box PCT
50 Victoria Street
Gatineau, Quebec K1A 0C9
Facsimile No.: 001-819-953-2476

Authorized officer
Bryon Braymore (819) 934-6753

INTERNATIONAL SEARCH REPORT

International application No.
PCT/CA2012/050206

Box No. II Observations where certain claims were found unsearchable (Continuation of item 2 of the first sheet)

This international search report has not been established in respect of certain claims under Article 17(2)(a) for the following reasons :

1. [ ] Claim Nos. :
   because they relate to subject matter not required to be searched by this Authority, namely :

2. [X] Claim Nos. : 53
   because they relate to parts of the international application that do not comply with the prescribed requirements to such an extent that no meaningful international search can be carried out, specifically :

   Omnibus claims are unsearchable because they fail to explicitly recite any particular feature.

3. [ ] Claim Nos. :
   because they are dependent claims and are not drafted in accordance with the second and third sentences of Rule 6.4(a).

Box No. III Observations where unity of invention is lacking (Continuation of item 3 of first sheet)

This International Searching Authority found multiple inventions in this international application, as follows :

1. [ ] As all required additional search fees were timely paid by the applicant, this international search report covers all searchable claims.

2. [ ] As all searchable claims could be searched without effort justifying additional fees, this Authority did not invite payment of additional fees.

3. [ ] As only some of the required additional search fees were timely paid by the applicant, this international search report covers only those claims for which fees were paid, specifically claim Nos. :

4. [ ] No required additional search fees were timely paid by the applicant. Consequently, this international search report is restricted to the invention first mentioned in the claims; it is covered by claim Nos. :

Remark on Protest [ ] The additional search fees were accompanied by the applicant's protest and, where applicable, the payment of a protest fee.

[ ] The additional search fees were accompanied by the applicant's protest but the applicable protest fee was not paid within the time limit specified in the invitation.

[ ] No protest accompanied the payment of additional search fees.

Patent Document Cited in Search Report	Publication Date	Patent Family Member(s)	Publication Date
EP1112459A1	04 July 2001 (04-07-2001)	AT540262T	15 January 2012 (15-01-2012)
		AU4645699A	14 February 2000 (14-02-2000)
		DK1112459T3	16 April 2012 (16-04-2012)
		EP1112459A4	09 June 2004 (09-06-2004)
		EP1112459B1	04 January 2012 (04-01-2012)
		ES2380322T3	10 May 2012 (10-05-2012)
		IL125412D0	30 April 2001 (30-04-2001)
		IL125412A	20 November 2005 (20-11-2005)
		WO0005536A1	03 February 2000 (03-02-2000)